Experimental evaluation and modeling of the hydrodynamics in structured packing operated with viscous waste oils

Margaux Lhuissier, Annabelle Couvert, Abdoulaye Kane, Abdeltif Amrane, Jean-Luc Audic, Pierre-Francois Biard

Experimental evaluation and modeling of the hydrodynamics in structured packing operated with viscous waste oils

Margaux Lhuissier[a], Annabelle Couvert[a], Abdoulaye Kane[b], Abdeltif Amrane[a], Jean-Luc Audic[a], Pierre-François Biard[a]

[a]Univ Rennes, Ecole Nationale Supérieure de Chimie de Rennes, CNRS, ISCR - UMR 6226, F-35000 Rennes, France

[b]UniLaSalle-Ecole des Métiers de l'Environnement, Campus de Ker Lann, 35170 Rennes, France

Graphical abstract:

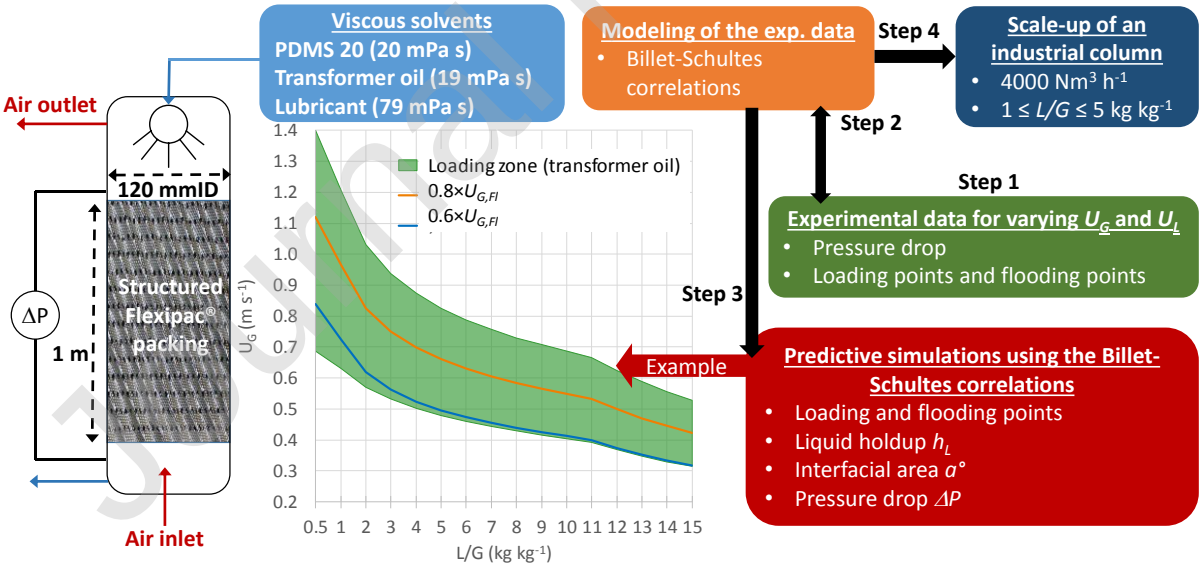

Highlights:

- Hydrodynamics of two waste oils and PDMS in a structured packing was investigated
- Pressure drop in the loading zone was lower than 450 Pa m^{-1}
- Loading and flooding velocities were relatively low, especially using the viscous lubricant
- Billet-Schultes correlations were efficient to predict the loading and flooding points and the pressure drop
- Scale-up calculations proved that transformer oil can be used in an industrial scale packed column

Abstract :

The purpose of this work was to study the hydrodynamic behavior of two viscous waste oils (a transformer oil and a lubricant characterized by viscosities of 19 mPa s and 79 mPa s, respectively) and a silicone oil (20 mPa s) in a laboratory-scale packed column (D_{col} = 0.12 m). The column was filled with structured packing made of corrugated sheets (Flexipac® 500Z HC) and was operated at counter-current. Thus, the gas superficial velocities at the loading point were in the range from 0.40 to 0.65 m s^{-1} for liquid loads between 1 and 24 m^3 m^{-2} h^{-1}, and, at the flooding point from 0.56 to 1.07 m s^{-1} for liquid loads between 6 and 36 m^3 m^{-2} h^{-1}. Both loading and flooding points were particularly influenced by the solvent viscosity, leading to a narrow loading zone for the most viscous solvent (lubricant). The pressure drop values remained reasonable, lower than 450 Pa m^{-1} in the loading zone, even for the lubricant. Billet-Schultes correlations were used for the prediction of the loading and flooding velocities and of the pressure drop. The specific constants of the model were determined. These correlations enable accurate predictions of the loading and flooding points, with an average relative error around 7-8%, and of the pressure drop in the loading zone, with an average relative error of 15%. Simulations were performed with the Billet-Schultes correlations and showed that high liquid holdup and interfacial area would be obtained with these viscous solvents in the selected packing. Scale-up calculations proved that it would be possible to implement the transformer oil at industrial scale in a packed column filled with the studied structured packing.

Keywords: Absorption; Hydrodynamics; waste oils; PDMS; packed column; modeling

Nomenclature

a: specific surface area of packing ($m^2\ m^{-3}$)

a_h : *hydraulic* surface area (Eq. 6 and Eq. 7, $m^2\ m^{-3}$)

$a°$: interfacial area relative to the packing volume ($m^2\ m^{-3}$)

ARE: Average Relative Error

C_P, C_{Lo}, C_{Fl}, C_h : constants relative to each commercial packing according to Billet-Schultes

d_h: hydraulic diameter = $4\varepsilon/a$ (m)

D_{col} : column diameter (m)

F: volume flowrate ($m^3\ h^{-1}$ or $m^3\ s^{-1}$)

g: specific gravity constant (9.81 m s^{-2})

G: gas mass flowrate (kg s^{-1})

h_L: liquid holdup (-)

L: liquid mass flowrate (kg s^{-1})

Re: Reynolds number (-)

U: superficial velocity (m s^{-1})

Z: packing height (m)

RE: Relative error

Greek letters

$\Delta P/Z$: Linear pressure drop (Pa m^{-1})

ε: Packing void fraction (-)

Ψ: resistance coefficient (-)

μ: dynamic viscosity (Pa s)

ρ: density (kg.m^{-3})

Subscripts

L: Relative to the liquid phase

G: Relative to the gas phase

Lo: At the loading point

Fl: At the flooding point

1. Introduction

Volatile Organic Compounds (VOCs) have harmful effects on the environment through their global warming contribution. Disturbing the Chapman cycle in the atmosphere by reacting with radicals, VOCs cause tropospheric ozone accumulation and thus intensify global warming (Le Cloirec, 2004). Besides, some VOCs could be toxic towards human health. Their impact on liver, blood and nervous systems have been demonstrated (Kampa and Castanas, 2008).

Several mature technologies can be implemented to remove VOCs from air such as adsorption on activated carbon filters, thermal and catalytic oxidations, absorption (gas-liquid scrubbing) or biofiltration (Ruddy and Carroll, 1993). To target hydrophobic VOCs, absorption in a non-aqueous phase (NAP) using silicone oils, phtalates, adipates or even ionic liquids, would be a promising treatment (Hadjoudj *et al.*, 2004; Heymes *et al.*, 2006; Bourgois *et al.*, 2006, 2009; Darracq *et al.*, 2010a; Darracq *et al.*, 2010b; Guihéneuf *et al.*, 2014; Biard *et al.*, 2016, 2018; Rodriguez Castillo *et al.*, 2018, 2019). Nonetheless, all these commercial or laboratory made solvents are very expensive, which would increase the CAPEX of an industrial process. Consequently, several studies have

recently investigated the potential of cheaper NAP, such as waste oils (Bay *et al.*, 2006; Lalanne *et al.*, 2008; Ozturk and Yilmaz, 2006).

In a previous paper investigating the physico-chemical properties (viscosity, volatility, partition coefficient for toluene and dichloromethane) of several industrial waste oils (Lhuissier *et al.*, 2018), lubricant and transformer oil were proved to be potential NAP candidates for VOC absorption. Nevertheless, these waste oils are from 10 to 70 times more viscous than water and have a low surface tension, which can affect significantly their hydrodynamics, especially in irrigated packed columns which are the most commonly used contactors at industrial scale for gas scrubbing (Le Cloirec, 2004; Minne, 2017).

In a counter-current packed column, it is recommended to operate in the loading zone located between the loading and flooding points (Billet and Schultes, 1999). Indeed, for gas velocities below the loading points (in the pre-loading zone), the downward flow of liquid, and consequently the liquid holdup, depend only on the liquid rate and are not influenced by the gas velocity, leading to low interfacial area and gas-liquid interactions (Billet and Schultes, 1999, 1995, 1993; Heymes *et al.*, 2006; Mackowiak, 2010; Stichlmair *et al.*, 1989). In this pre-loading zone, the pressure drop increases linearly with the gas superficial velocity (Piché *et al.*, 2001a). In the loading zone, the shear forces in the gas flow support some of the descending liquid allowing to increase advantageously the liquid holdup and the interfacial area (Billet and Schultes, 1999; Piché *et al.*, 2001a). In the loading zone, the pressure drop increases with the gas superficial velocity to a power of around 1.8 (Piché *et al.*, 2001a). Then, when the flooding point is reached, the shear stress of the gas flow is high enough to maintain the liquid at the top of the column, *i.e.* the liquid starts to overflow and the pressure drop increases sharply (Billet and Schultes, 1999, 1995, 1993; Piché *et al.*, 2001b). Consequently, for a given gas flowrate, the choice of a working point in the loading zone allows subsequently to determine the diameter of the contactor (Roustan, 2003). More precisely, a working gas superficial velocity equal to 70-80% of the flooding velocity is recommended by several authors (Billet and Schultes, 1999; Maćkowiak, 1991), even if a lower boundary of 60% was also proposed (Roustan, 2003).

Several semi-empirical correlations have been developed in the literature to determine the loading and flooding points as-well-as liquid holdup and pressure drop in the pre-loading and loading zones of either random and structured packing (Maćkowiak, 1990, 1991; Miyahara *et al.*, 1992; Rocha *et al.*,

1993; Billet and Schultes, 1999; S. Piché *et al.*, 2001a, 2001b, 2001c; Heymes *et al.*, 2006). These correlations take into account the column diameter, packing characteristics (porosity, particle diameter, specific surface area, etc.), liquid and gas properties (viscosity, density, superficial tension) and liquid-to-gas mass flowrate ratio *L/G*. Besides, the pressure drop in the loading zone depends also on the selected liquid and gas velocities. Most of these correlations were established using data gathered with water-like solvents having low or moderate viscosities. The Billet-Schultes correlations were developed in the 90^{ties} for both random and structured packing with solvents having dynamic velocities up to around 100 mPa s (Billet and Schultes, 1999, 1993). In 2006, Heymes *et al.* showed that these correlations were the most accurate to predict the pressure drop of dumped packing using DEHA. In 2017, Minne also proved the good predictive capacity of these correlations using solvents with different viscosities, densities and surface tension (ethylene glycol, silicone oil, water and Isopar G). The procedure developed by Billet-Schultes involves the calculation of liquid holdup, which is the ratio of the liquid within the column volume to the packing volume.

Only a few studies have been performed to assess the hydrodynamics of viscous solvents in packed columns, and up to now, no one has been dedicated to waste oils (Brunazzi *et al.*, 2002; Darracq, 2011; Guillerm *et al.*, 2016; Heymes *et al.*, 2006; Minne, 2017; Minne *et al.*, 2018; Tsai *et al.*, 2009). Thus, the purpose of this work is to study the hydrodynamics of two waste oils, a lubricant and a transformer oil, in a laboratory scale packed column, by comparison to another reference solvent: a commercial silicone oil (PDMS 20). A modern 4th generation structured packing made of metallic corrugated sheets was used (Flexipac® 500Z HC). Both the loading and flooding points for several liquid-to-gas mass flowrate ratios (L/G) have been determined, as well as the pressure drop evolution with the gas and liquid velocities. Besides, the reliability of the Billet-Schultes correlations was evaluated allowing to subsequently simulate different conditions and to assess the scale-up of the process at industrial scale.

2. Material and method

2.1 Chemical products

The silicone oil used was composed of polydimethylsiloxane (PDMS), a synthetic oil named Rhodorsil 47V20 provided by Bluestar Silicones (Table 1). The waste oils were selected among those collected by Chimirec (Javené, France).

2.2 Pilot-scale packed column

The irrigated packed column (120 mmID (D_{col}) and packing height Z of 1 m) was operated at counter current (Fig. 1). The air flow (ρ_G = 1.17 kg m^{-3} at 25°C and 1 atm) was introduced at the bottom of the column and the liquid solvent was introduced at the top of the column. The column was filled with structured packing (Flexipac®, provided by Koch Glitsch-USA) made out of corrugated sheets arranged in a crisscrossing configuration to create flow channels for the gas phase (Table 2).

The air flowrate was regulated by means of a membrane valve located after a fan and measured by a rotameter (GF Type SK 20 CH-8201, Switzerland). The column was fed with the liquid absorbent by means of a centrifugal pump (Iwaki MD100, Japan). The liquid flowrates were regulated with a valve and measured by a previously calibrated rotameter (GF type SK 11 CH-8201, Switzerland). The experimental conditions and the range of operating parameters are shown in Table 3. For each liquid flowrate selected, the gas flow was increased incrementally up to the flooding point (determined by visual observation), and pressure drops (ΔP) were measured three times for each point using a vertical U-shaped tube filled with water. Only the pressure drop corresponding to the packing was measured. The temperature of the liquid phase ranged from 294 to 298 K, and the gas temperature was kept constant at 298 K by means of a heat exchanger. Considering all the experiments, the difference between the inlet temperatures of the gas and liquid phases was always lower than 3 K. The accuracy and reliability of this set-up was previously checked by Darracq and Guillerm (Darracq, 2011; Guillerm, 2017).

Billet-Schultes correlations

Billet and Schultes (B-S) developed a set of correlations allowing to determine (i) both the loading and flooding gas superficial velocities ($U_{G,Lo}$ and $U_{G,Fl}$) for a given L/G ratio and (ii) the pressure drop, liquid holdup and the interfacial area for the selected working gas superficial velocity (U_G) in both the pre-loading and loading zones (Billet and Schultes, 1999, 1995, 1993, 1991). These correlations, presented in Table 4, involve several constants which depend specifically on the packing (C_P, C_{Lo}, C_{Fl} and C_h). The structured packing used in this study was not previously tested by Billet-Schultes.

Therefore, the constants used in our calculations were deduced from the experimental results (part 3.3). For a given packing, the loading and flooding points depend on the selected *L/G* ratio, the liquid and gas properties and the packing properties. They can be deduced from the equations 1-7 and 8-11, respectively. These sets of equations need to be solved by iteration (for example using the Excel® Solver). The determination of the loading points involved the determination of the ratio of the hydraulic to the geometric surface area (a_h/a) according to Eqs. 6 or 7. This ratio must not be confused with the ratio of the specific interface between the phases to the geometric area ($a°/a$), determined with Eqs. 18-20. Besides, these equations involve several resistance coefficients (Ψ) whose calculation depends on the nature of the dispersed phase (Eqs. 3-4 and Eqs. 10-11).

3. Results and Discussion

3.1 Experimental pressure drop of the irrigated column

The experimental pressure drop of the irrigated packed column increases logically with both the liquid and gas superficial velocities according to Fig. 2. The gas velocity can be easily converted to the vapor capacity factor F_V, often used to report data dealing with the hydrodynamics of an irrigated packed column (Minne, 2017), by multiplication with the square root of the air density (which was almost constant in this study and equal to 1.17 kg m^{-3}). Lower liquid velocities were applied for the lubricant since the flooding was reached at a lower *L/G* ratio for a given gas velocity than for silicon and transformer oils. This observation is consistent with the fact that both loading and flooding points appear at lower gas velocities for viscous solvents at similar liquid densities (Minne, 2017). Nonetheless, even with a high viscosity, it would be feasible to use this lubricant in a packed column.

In Fig. 2, experimental points located in both pre-loading and loading zones are represented. Some values of the pressure drop were also measured in the flooding zone but are not represented in Fig. 2 for clarity. In the pre-loading zone, the pressure drop increases linearly with the gas velocity and is minimally influenced by the nature and the flowrate of the liquid. Minne (2017) and Brunazzi *et al.* (2002) also observed this behavior for various liquids with similar densities but very different viscosities for random and structured packing, respectively. It is consistent with the fact that gas and liquid have almost no interaction in the pre-loading zone. However, this behavior completely changes

when the loading point is reached. Indeed, the pressure drop at given liquid and gas velocities is significantly higher for the lubricant in the loading zone than for the transformer oil and the silicon oil. Furthermore, the pressure drop increases with the gas velocity to the power of 1.8. All these observations in the loading zone are in agreement with the literature (Minne, 2017; Minne *et al.*, 2018; Piché *et al.*, 2001a). The results emphasize that the pressure drop values stay advantageously under 450 $Pa.m^{-1}$ in both the pre-loading and loading zones for each of the viscous liquid phases, showing that the implementation of viscous solvents would not affect significantly the operating costs (OPEX). However, the results clearly show that lower *L/G* ratios must be selected when the solvent viscosity increases to avoid loading and flooding points that would be too low, highlighting that the determination of the loading and flooding points would be determinant when designing a column. To reach this goal, robust models must be implemented.

3.2 Determination of the experimental loading and flooding points

The log-log plots corresponding to Fig. 2 are provided as supplementary material (Fig S.1). For the three solvents, the experimental loading and flooding superficial velocities, summarized in Table 5 and Table 6, were determined from the break-up of the slopes between the pre-loading zone, the loading zone and the flooding zone on these log-log plots.

The loading and flooding points for a given liquid-to-gas mass flowrate ratio (*L/G*) were close to the results obtained previously by Guillerm *et al.* (2016) with the same packing using PDMS 50 (viscosity of 50 mPa.s). The observed loading and flooding velocities are relatively low, in the range 0.39-0.65 and 0.56-1.06 m s^{-1}, respectively. This behavior is justified by both the nature of the packing, which is a structured packing with a high interfacial area leading to a high liquid capacity, and the high viscosity of the solvents investigated.

Indeed, in agreement with the experimental observations and theoretical considerations of other authors (Billet and Schultes, 1995; Brunazzi *et al.*, 2002; Minne *et al.*, 2018), both loading and flooding velocities decreased with the solvent viscosity because of higher frictional forces. Thus, lower liquid loads were operated for the most viscous solvent, *i.e.* the lubricant. Nonetheless, having similar

viscosities, densities and surface tensions, the loading and flooding velocities for the transformer oil and the silicon oil are not significantly different at a given liquid load. On the one hand, the influence of the density on the hydrodynamics is rather well described in the literature. Indeed, the gravitational forces are counterbalanced by the frictional forces at lower velocities when the density decreases (Minne, 2017). On the other hand, the possible influence of the surface tension is still controversial in the literature and seems to depend on the nature of the packing and of the liquid load (Minne, 2017). Anyway, the Billet-Schultes model, applied in the next part, does not take the influence of the surface tension into account.

3.3 Application of the Billet-Schultes: determination of the specific constants for Flexipac® 500Z HC packing.

Eqs 8-11 show that the determination of the flooding point at a given *L/G* ratio depends on the properties of the liquid phase (viscosity μ and density ρ) and on the properties and the nature of the packing through its void fraction ε, specific area *a* and through a specific constant C_{Fl}. By trying to minimize the sum of the relative errors (*RE*) between the experimental gas flooding velocities and those deduced from the B-S correlations, the value of C_{Fl} was determined (Table 7). The value found is in agreement with the range previously determined by Billet and Schultes (Billet and Schultes, 1999). The low average relative error (*ARE*) of 7.5% (calculated for 11 values) between the experimental and theoretical gas flooding velocities (summarized on Table 6) shows that B-S correlations are efficient for the prediction of the flooding points even for solvents with very different properties. Minne (2017) found similar *RE* for a silicon oils using two dumped packing. The parity plot is provided as supplementary material and does not put in evidence any systematic error (Fig. S-2(b)). From Eqs 8-11, the liquid holdup at the flooding points was also determined (Table 6).

Eqs. 1-7 show that the determination of the loading point at a given *L/G* ratio depends on the properties of the liquid phase (viscosity μ and density ρ) and on the properties and the nature of the packing through its void fraction ε, specific area *a* and through two specific constant C_{Lo} and C_h. Several couples (C_{Lo} ;C_h) allowed to minimize the *ARE* between the experimental gas loading velocities and those deduced from the B-S correlations. Thus, the best couple summarized on Table 7 was determined through the simultaneous minimization of the *ARE* of both the experimental and theoretical pressure drops and loading points. Only the pressure drops measured in the loading zone

were considered. Indeed, the pressure drop in the pre-loading zone is low and suffers from higher experimental uncertainties. Besides, Minne (2017) pointed out the relatively low performance of the Billet-Schultes model to predict the pressure drop on the pre-loading zone.

The values of C_h and C_{Lo} found are in agreement with the ranges previously determined by Billet and Schultes (Billet and Schultes, 1999), even if the value of C_{Lo} is slightly lower than the range of Table 7. The low *ARE* of 8.0% (calculated for 10 values) between the experimental and theoretical gas loading velocities (summarized on Table 5) shows that the B-S correlations are efficient for the prediction of the loading points, even for solvents with very different properties. The parity plot is provided as supplementary material and shows that the model slightly overestimates the loading points for the lubricant and slightly underestimates them for the transformer oil (Fig. S-2(a)), but these discrepancies remain acceptable.

The results summarized in Table 5 and Table 6 clearly confirm that the liquid holdup would be higher at a given *L/G* ratio for the lubricant, *i.e.* for a higher viscosity, for both the loading and flooding points. Thus, even if viscous solvents must be operated at a lower superficial gas velocity and/or a lower *L/G* ratio (*i.e.* lower absorption rate (Biard *et al.*, 2018)), a higher interfacial area would be expected.

Finally, the value of C_p (Table 7) was determined through the minimization of the *ARE* between the experimental and theoretical (Eqs 12-17) pressure drops of the points located in the loading zones. The value of C_p found is in agreement with the range previously determined by Billet and Schultes (Billet and Schultes, 1999). The low average relative error of 15.1% (calculated for 134 values: 42 for PDMS 20, 32 for transformer oil, 60 for lubricant) between the experimental and theoretical pressure drops in the loading zone shows that B-S correlations estimate with a good confidence level the pressure drop even with viscous solvents. On the pre-loading zone, the agreement is lower, with an *ARE* of 34.1%, which is consistent with the observations of Minne (2018). Nonetheless, it is not recommended to operate on the pre-loading zone (Billet and Schultes, 1999). The agreement between the experimental and theoretical pressure drops on the pre-loading and loading zones can be assessed Fig. 2. The detailed *ARE* for the three solvents in each zone are summarized in Table 8. It shows that the best agreement is found for PDMS 20 and transformer oil. For the lubricant, the *ARE* is higher, around 27%, but remains fully acceptable. Furthermore, the parity plot of the pressure drop is provided as supplementary material and does not put in evidence any systematic error (Fig. S-3).

3.4 Discussion and simulations

From the constants determined previously (Table 7) and the B-S correlations, it was possible to estimate the loading and flooding points for the two waste oils for an increasing *L/G* ratio in the 0.5-15 range (Fig. 3).

The loading and flooding velocities obviously decrease with the *L/G* ratio. For the lubricant (*i.e.* the most viscous solvent), the loading velocity is from 6% (at *L/G* = 0.5) to 20% higher (at *L/G* = 15) and the flooding velocity is from 10% (at *L/G* = 0.5) to 30% higher (at *L/G* = 15) than for the transformer oil. Because of almost identical properties, the data for PDMS 20 are similar to those of the transformer oil and are not represented. For the sake of comparison, a simulation for water was also carried out (Fig. S-4). The results show that for this solvent, the loading and flooding points would be respectively from 17 to 52% higher and from 25 to 48% higher than for the transformer oil.

Fig. 3 shows that the choice of a working velocity at 80% of the flooding velocity allows operating in the loading zone in any case. However, the choice of a working velocity at 60% of the flooding velocity, proposed as a lower boundary by some authors (Roustan, 2003), would be inappropriate, especially at high *L/G* ratio and for the lubricant. The breakthrough of the curves observed at a *L/G* ratio around eleven is due to a shift of the dispersed phase (from the liquid to the gas phase) corresponding to a value of $\frac{L}{G} \times \sqrt{\frac{\rho_G}{\rho_L}}$ higher than 0.4 (Table 4).

Fig. 3 also highlights that the selection of an excessive *L/G* ratio would be inappropriate for several reasons. Indeed, for the viscous solvents investigated, it would impose to select a low superficial gas velocity, *i.e.* to increase the column diameter for a given gas flowrate to treat. Moreover, a low superficial gas velocity would affect the turbulences in the gas phase, decreasing the gas-phase mass transfer rate. Since a significant part of the mass transfer resistance can be located in the gas phase during hydrophobic VOC absorption, even using viscous solvents (Biard *et al.*, 2018; Rodriguez Castillo *et al.*, 2019), would decrease the overall mass transfer rate. Finally, for a high *L/G* ratio, the loading zone is narrower. Thus, low variations of the gas velocity may induce significant variations of the hydrodynamics within the column, which would complicate the monitoring of a packed column at industrial scale.

The evolution of the pressure drop $\Delta P/Z$ (orange curves), the liquid holdup h_L (yellow curves) and the ratio $a°/a$ was simulated for several liquid loads (Fig. 4). h_L and the ratio $a°/a$ remain constant in the pre-loading zone in agreement with the experimental observations of several authors with structured packing (Billet and Schultes, 1993; Brunazzi *et al.*, 2002; Zakeri *et al.*, 2012). In the pre-loading zone, h_L and the ratio $a°/a$ increase by 100% for the transformer oil when the liquid load increases by a factor of 4 (from 5 to 20 m h^{-1}). Moreover, h_L and the ratio $a°/a$ are around 30% higher for the lubricant in the pre-loading zone. Brunazzi *et al.* (2002) also showed that the liquid holdup increases with the solvent viscosity even in the pre-loading zone. Thus, a viscous solvent exhibits advantageously a higher interfacial area although the pressure drop is almost insensitive to the nature of the solvent, at least in the pre-loading zone.

When the loading zone is reached (around 0.60 m s^{-1} for U_L = 5 m h^{-1} and around 0.45 m s^{-1} for U_L = 20 m h^{-1} for the transformer oil; around 0.55 m s^{-1} for U_L = 5 m h^{-1} for the lubricant), the gas and the liquid start to interact. Thus, both h_L and the ratio $a°/a$ increase until the flooding point is reached (around 1.20 m s^{-1} for U_L = 5 m h^{-1} and around 0.78 m s^{-1} for U_L = 20 m h^{-1} for transformer oil; around 1.02 m s^{-1} for U_L = 5 m h^{-1} for the lubricant). A rather high liquid holdup, from 25 to more than 45%, would be reached at the flooding point. High liquid hold ups are concomitant with a good wetting of the column and with high interfacial area $a°$. The interfacial area can be even higher that the geometrical area a of the packing according to the experimental observations of Tsai *et al.* (2009) on similar structured packing fed with solvents having viscosities up to 14 mPa s. Cherif *et al.* (2017) showed the good predictive capacity for $a°$ of the Billet-Schultes correlations for a structured packing. In the loading zone, contrarily to the pre-loading zone, the pressure drop is particularly sensitive to the liquid load and the viscosity of the solvent. Thus, for example, at a liquid load of 5 m h^{-1} and a gas velocity of 0.8 m s^{-1}, the interfacial area and the pressure drop for the lubricant would be around 40% and 15% higher than for the transformer oil, respectively.

3.5 Packing scale-up

According to part 3.3, the Billet-Schultes correlations provide fair estimations of the pressure drop and loading and flooding points. These parameters are crucial for the evaluation of the operating cost through the determination of the packed column diameter and the selection of the *L/G* ratio (part 3.4).

In this part, in order to study the scale-up of a column with this specific packing, a realistic case involving a flowrate of 4000 $Nm^3.h^{-1}$ of air to be treated was considered (where N stands for the standard temperature and pressure (STP) conditions, meaning 1 bar and 0°C according to the IUPAC). The transformer oil was selected among the three solvents considering the observations of the parts 3.3 and 3.4. Biard *et al.* (Biard *et al.*, 2018; Rodriguez Castillo *et al.*, 2019) already studied the hydrodynamics of DEHA (12.5 mPa s), PDMS (50 mPa s) and two ionic liquids (50-60 mPa s) in a packed column (D_{col} = 1 m) filled with bulk Pall® rings for with the same gas flowrate using the Billet-Schultes correlations. Apart from a different packing nature (corrugated sheets vs. random rings), Pall® rings offer a geometric surface area of only 139.4 $m^2\ m^{-3}$, around 3 times lower than Flexipac®500 Z HC. Thus, both the computed loading and flooding superficial velocities for similar *L/G* ratio (in the range 1-5) are significantly lower with the Flexipac® packing. Thus, it was impossible to select the same working velocity of 1.52 m s^{-1} as Biard *et al.* (Biard *et al.*, 2018; Rodriguez Castillo *et al.*, 2019) since this one is higher than the computed flooding velocity for the Flexipac® packing whatever the *L/G* ratio considered.

Thus, for this scale-up assessment, a *L/G* ratio in the range 1-5 to avoid flooding velocities that were too low (Fig. 3 (a)) was selected. Then, a working gas velocity taken at 80% of the flooding velocity as recommended in the literature was considered (Billet and Schultes, 1999). A working gas velocity (which decreases with the *L/G* ratio), in the range 0.54-0.86 m s^{-1}, and a column diameter (which increases with the *L/G* ratio), in the range 1.33-1.68 m, were calculated. Fig. 5 presents the evolution of the liquid holdup h_L, interfacial area $a°$ and pressure drop $\Delta P/Z$ calculated with the B-S correlations for increasing *L/G* ratios.

The calculated pressure drops would be in a reasonable range (95-175 Pa m^{-1}) for an industrial application. The pressure drop would be lower at industrial scale at given liquid and gas velocities than at the lab-scale, because of negligible wall effects. These wall effects are taken into account by the Billet-Schultes correlations through the column diameter (Eqs. 15-17). The pressure drop decreases with the *L/G* ratio and with the working gas velocity U_G, even if the liquid holdup and the liquid load

increase. The low values of the pressure drop must be balanced with the low gas velocity tolerated by this packing. It confirms that viscous solvents do not necessarily lead to high pressure drop (Biard *et al.*, 2018). Advantageously, the computed interfacial area is significant, higher than 200 m^2 m^{-3}. These results emphasize the good hydrodynamic performance offered by this packing. Nonetheless, the use of a low gas velocity would be detrimental for the mass transfer rate in the gas phase, in which the main part of the resistance can be located, especially during the absorption of hydrophobic VOCs for which the selection of viscous absorbents is justified (Rodriguez Castillo *et al.*, 2019).

4. Conclusion

The purpose of this work was to study the hydrodynamic behavior of two viscous waste oils (a transformer oil and a lubricant characterized by viscosities of 19 mPa s and 79 mPa s, respectively) and a silicone oil (20 mPa s) in a laboratory-scale packed column (D_{col} = 0.12 m) filled with structured packing (Flexipac® 500Z HC). First, the results showed that it was possible to successfully apply such viscous solvents in structured packing made of corrugated sheets. The loading and flooding points were determined for *L/G* ratios between 0.3 and 14.0. Pressure drop in the loading zone values were in the range from 50 to 450 $Pa.m^{-1}$. The pressure drop values were significantly higher in the loading zone at the same gas and liquid velocities for the most viscous solvent (lubricant) than for the other solvents. Besides, lower liquid loads (*i.e*. liquid velocities) must be applied for the lubricant, since the flooding point was reached at lower gas velocities for a given *L/G* ratio. Considering that the high lubricant viscosity will also lower the mass transfer rate (directly, through lower turbulences, and indirectly, through lower diffusion coefficients (Rodriguez Castillo *et al.*, 2019)), the selection of such a viscous solvent would be justified only for pollutant/solvent systems characterized by low partition coefficient (*i.e.* high affinities).

In order to apply waste oils in a scrubbing process, the accurate prediction of the hydrodynamic performance is a prerequisite. The Billet-Schultes correlations (Billet and Schultes, 1999) were used to predict the loading points and flooding points, as well as the pressure drop, the liquid holdup and the interfacial area at the working velocity. The specific constants of the packing used were determined by numerical resolution. The *ARE* between the experimental and theoretical pressure drops in the loading

zone was around 15%. Furthermore, the Billet-Schultes correlations successfully determined the loading and flooding points with *ARE* around 7-8%. Several simulations were performed with these correlations to assess the influence of the operating conditions. It highlighted the high hydrodynamic performance of this packing. It also demonstrated that the use of viscous solvents does not necessarily lead to excessive pressure drop in agreement with the experimental results. *A fortiori*, high liquid holdup and interfacial area would be advantageously obtained. Nonetheless, low loading and flooding velocities were computed, even for a low *L/G* ratio, which leads to select low working gas velocities, leading to high diameter columns and lowered mass transfer rate in the gas phase. Finally, the scale-up of a realistic packed column for gas treatment was assessed and showed that that it would be possible to apply these kinds of solvents with the Flexipac®500Z HC packing even at industrial scale. For a complete techno-economic assessment, the determination of the mass transfer coefficients in both the liquid and gas phases will be necessary, allowing to evaluate concomitantly the pressure drop, the overall mass transfer coefficient and thus, the resulting removal efficiency in a given packed column (Biard *et al.*, 2018; Rodriguez Castillo *et al.*, 2019).

5. Acknowledgments

We are very grateful to the French Association Nationale de la Recherche et de la Technologie (ANRT) for the CIFRE PhD grant N° 2016/0238 attributed to Margaux Lhuissier, and also to the French governmental agency ADEME for the CORTEA funding n°1881C0001. We would like to thank our industrial partner Chimirec for providing the waste oils used in this study. We would like to give a warm thanks to Thomas HULL (UniLaSalle-Ecole des Métiers de l'Environnement) for proofreading this article.

Declaration of interests

The authors declare that they have no known competing financial interests or personal relationships that could have appeared to influence the work reported in this paper.

References

Aluyor, E.O., Ori-Jesu, M., 2009. Biodegradation of mineral oils–A review. African Journal of Biotechnology 8.

Bay, K., Wanko, H., Ulrich, J., 2006. Absorption of Volatile Organic Compounds in Biodiesel. Chemical Engineering Research and Design 84, 22–28.

Biard, P.-F., Coudon, A., Couvert, A., Giraudet, S., 2016. A simple and timesaving method for the mass transfer assessment of solvents used in physical absorption. Chemical Engineering Journal 290, 302–311.

Biard, P.-F., Couvert, A., Giraudet, S., 2018. Volatile organic compounds absorption in packed column: theoretical assessment of water, DEHA and PDMS 50 as absorbents. J. Indus. Eng. Chem. 59, 70–78.

Billet, R., Schultes, M., 1999. Prediction of mass transfer columns with dumped and arranged packings: updated summary of the calculation method of Billet and Schultes. Chemical Engineering Research and Design 77, 498–504.

Billet, R., Schultes, M., 1995. Fluid dynamics and mass transfer in the total capacity range of packed columns up to the flood point. Chem. Eng. Technol. 18, 371–379.

Billet, R., Schultes, M., 1993. A physical model for the prediction of liquid hold-up in two-phase countercurrent columns. Chemical engineering & technology 16, 370–375.

Billet, R., Schultes, M., 1991. Modelling of pressure drop in packed columns. Chem. Eng. Technol. 14, 89–95.

Bourgois, D., Thomas, D., Fanlo, J.-L., Vanderschuren, J., 2006. Solubilities at High Dilution of Toluene, Ethylbenzene, 1,2,4-Trimethylbenzene, and Hexane in Di-2-ethylhexyl, Diisoheptyl, and Diisononyl Phthalates. Journal of Chemical & Engineering Data 51, 1212–1215.

Bourgois, D., Vanderschuren, J., Thomas, D., 2009. Study of mass transfer of VOCs into viscous solvents in a pilot-scale cables-bundle scrubber. Chemical Engineering Journal 145, 446–452.

Brunazzi, E., Paglianti, A., Spiegel, L., Tolaini, F., 2002. Hydrodynamics of a gas-liquid column equipped with MellapakPlus packing, in: International Conference on Distillation and Absorption.

Cherif, H., Coquelet, C., Stringari, P., Clodic, D., Toubassy, J., 2017. Comparison of models for the prediction of hydrodynamic parameters in structured packing columns for biogas purification.

Darracq, G., 2011. Couplage de l'absorption dans une phase organique et de la biodégradation dans un réacteur multiphasique. Application au traitement de Composés Organiques Volatils hydrophobes. PhD thesis ENSCR-005, Rennes.

Darracq, G., Couvert, A., Couriol, C., Amrane, A., Le Cloirec, P., 2010. Integrated process for hydrophobic VOC treatment-solvent choice. The Canadian Journal of Chemical Engineering 655–660.

Darracq, Guillaume, Couvert, A., Couriol, C., Amrane, A., Thomas, D., Dumont, E., Andres, Y., Le Cloirec, P., 2010. Silicone oil: An effective absorbent for the removal of hydrophobic volatile organic compounds. Journal of Chemical Technology & Biotechnology 85, 309–313.

Guihéneuf, S., Castillo, A.S.R., Paquin, L., Biard, P.-F., Couvert, A., Amrane, A., 2014. Absorption of Hydrophobic Volatile Organic Compounds in Ionic Liquids and Their Biodegradation in Multiphase Systems, in: Fang, Z., Smith, Jr., Richard L., Qi, X. (Eds.), Production of Biofuels and Chemicals with Ionic Liquids, Biofuels and Biorefineries. Springer Netherlands, Dordrecht, pp. 305–337.

Guillerm, M., 2017. Optimisation du couplage de l'absorption et de la biodégradation pour l'élimination de Composés Organiques Volatils hydrophobes (These de doctorat). Rennes, Ecole nationale supérieure de chimie.

Guillerm, M., Couvert, A., Amrane, A., Norrant, E., Lesage, N., Dumont, E., 2016. Absorption of toluene in silicone oil: Effect of the solvent viscosity on hydrodynamics and mass transfer. Chemical Engineering Research and Design 109, 32–40.

Hadjoudj, R., Monnier, H., Roizard, C., Lapicque, F., 2004. Absorption of Chlorinated VOCs in High-Boiling Solvents: Determination of Henry's Law Constants and Infinite Dilution Activity Coefficients. Industrial & Engineering Chemistry Research 43, 2238–2246.

Heymes, F., Manno Demoustier, P., Charbit, F., Louis Fanlo, J., Moulin, P., 2006. Hydrodynamics and mass transfer in a packed column: Case of toluene absorption with a viscous absorbent. Chemical Engineering Science 61, 5094–5106.

Kampa, M., Castanas, E., 2008. Human health effects of air pollution. Environmental Pollution, Proceedings of the 4th International Workshop on Biomonitoring of Atmospheric Pollution (With Emphasis on Trace Elements) 151, 362–367.

Lalanne, F., Malhautier, L., Roux, J.-C., Fanlo, J.-L., 2008. Absorption of a mixture of volatile organic compounds (VOCs) in aqueous solutions of soluble cutting oil. Bioresource Technology 99, 1699–1707.

Le Cloirec, P., 2004. COV (composés organiques volatils). Techniques de l'Ingénieur G1, 1–10.

Lhuissier, M., Couvert, A., Amrane, A., Kane, A., Audic, J.-L., 2018. Characterization and selection of waste oils for the absorption and biodegradation of VOC of different hydrophobicities. Chemical Engineering Research and Design 138, 482–489.

Mackowiak, J., 2010. Fluid Dynamics of Packed Columns - Principles of the Fluid Dynamic Design of Columns for Gas/Liquid and Liquid/Liquid Systems, VDI-Buch. Springer, Berlin Heidelberg.

Maćkowiak, J., 1991. Pressure drop in irrigated packed columns. Chemical Engineering and Processing: Process Intensification 29, 93–105.

Maćkowiak, J., 1990. Determination of flooding gas velocity and liquid hold-up at flooding in packed columns for gas/liquid systems - Maćkowiak - 1990 - Chemical Engineering & Technology - Wiley Online Library.

Minne, U.L., 2017. Effect of liquid and gas physical properties on the hydrodynamics of packed columns (Thesis). Stellenbosch : Stellenbosch University.

Minne, U.L., Burger, A.J., Schwarz, C.E., 2018. The effect of fluid properties and packing size on the hydrodynamics of packed columns. Chemical Engineering Transactions 69, 31–36.

Miyahara, T., Ogawa, K., Nagano, Y., Hirade, A., Takahashi, T., 1992. Flow dynamics in low height packed column having large fractional void space. Chemical engineering science 47, 3323–3330.

Ozturk, B., Yilmaz, D., 2006. Absorptive Removal of Volatile Organic Compounds from Flue Gas Streams. Process Safety and Environmental Protection 84, 391–398.

Piché, S., Larachi, F., Grandjean, B., 2001a. Improving the prediction of irrigated pressure drop in packed absorption towers. Can. J. Chem. Eng. 79, 584–594.

Piché, S., Larachi, F., Grandjean, B., 2001b. Loading Capacity in Packing Towers–Database, Correlations and Analysis. Chem. Eng. Technol. 24, 373–380.

Piché, S., Larachi, F., Grandjean, B., 2001c. Flooding capacity in packed towers: database, correlations, and analysis. Ind. Eng. Chem. Res. 40, 476–487.

Rocha, J.A., Bravo, J.L., Fair, J.R., 1993. Distillation columns containing structured packings: a comprehensive model for their performance. 1. Hydraulic models. Industrial & Engineering Chemistry Research 32, 641–651.

Rodriguez Castillo, A.S., Biard, P.-F., Guihéneuf, S., Paquin, L., Amrane, A., Couvert, A., 2019. Assessment of VOC absorption in hydrophobic ionic liquids: Measurement of partition and diffusion coefficients and simulation of a packed column. Chem. Eng. J. 360, 1416–1426.

Rodriguez Castillo, A.S., Guihéneuf, S., Biard, P.-F., Paquin, L., Amrane, A., Couvert, A., 2018. Physicochemical properties of some hydrophobic room-temperature ionic liquids applied to volatile organic compounds biodegradation processes: Physicochemical properties of some hydrophobic room-temperature ionic liquids. Journal of Chemical Technology & Biotechnology 93, 215–223.

Roustan, M., 2003. Transferts gaz-liquide dans les procédés de traitement des eaux et des effluents gazeux. Lavoisier, Paris.

Ruddy, E.N., Carroll, L.A., 1993. Select the best VOC control strategy. Chemical engineering progress 89, 28–35.

Stichlmair, J., Bravo, J.L., Fair, J.R., 1989. General model for prediction of pressure drop and capacity of countercurrent gas/liquid packed columns. Gas Separation & Purification 3, 19–28.

Tsai, R.E., Seibert, A.F., Eldridge, R.B., Rochelle, G.T., 2009. Influence of viscosity and surface tension on the effective mass transfer area of structured packing. Energy Procedia 1, 1197–1204.

Zakeri, A., Einbu, A., Svendsen, H.F., 2012. Experimental investigation of liquid holdup in structured packings. Chemical Engineering Research and Design 90, 585–590.

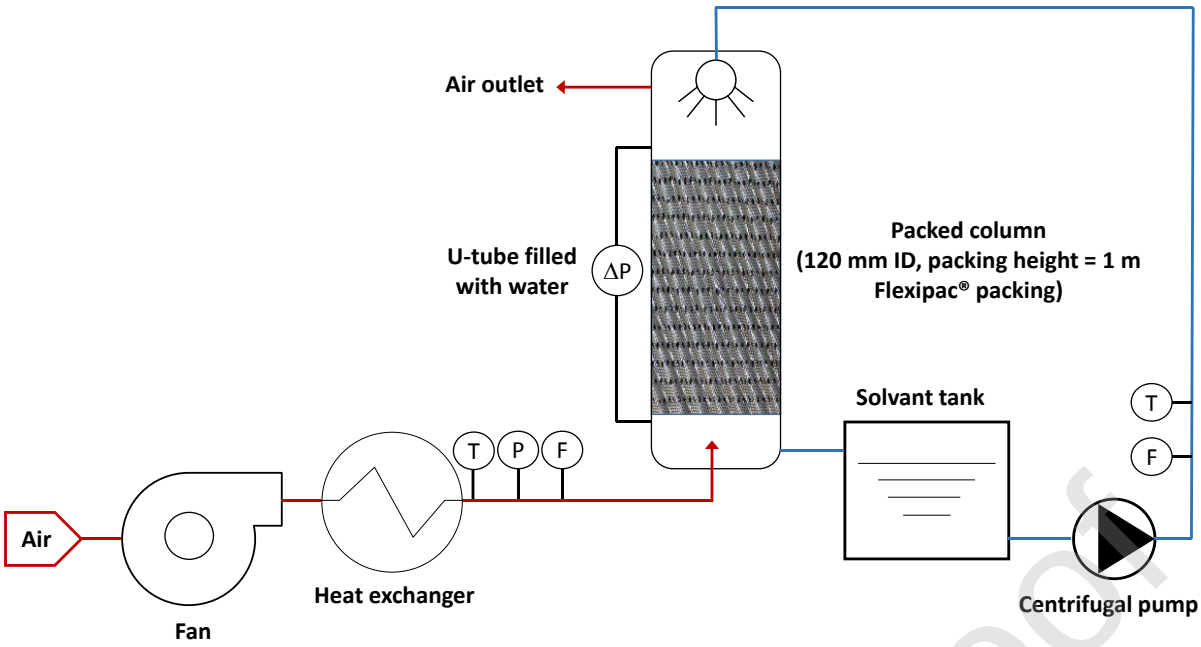

Figure 1: Experimental set-up.

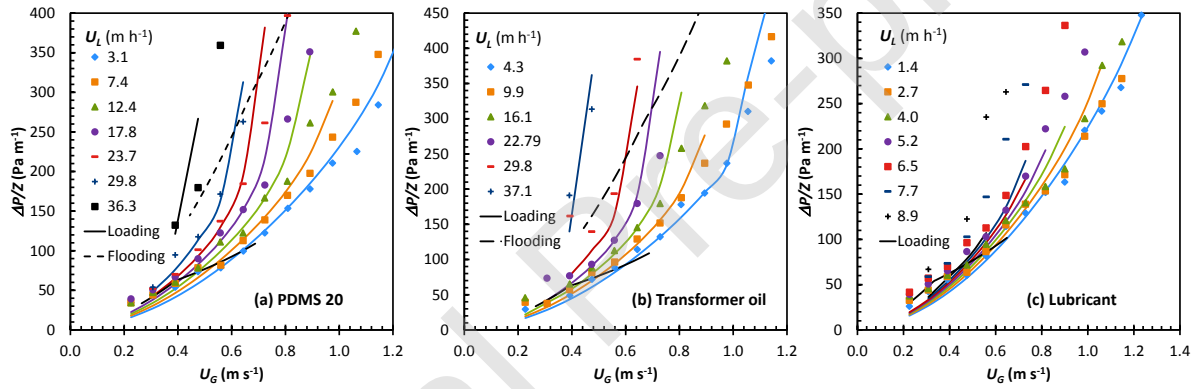

Figure 2 : Evolution of the pressure drop with the gas velocity for PDMS (a), transformer oil (b) and lubricant (c) for increasing values of the liquid load U_L (in m^3 m^{-2} h^{-1}). The straight lines correspond to the calculations according to the Billet-Schultes correlations (part 3.3).

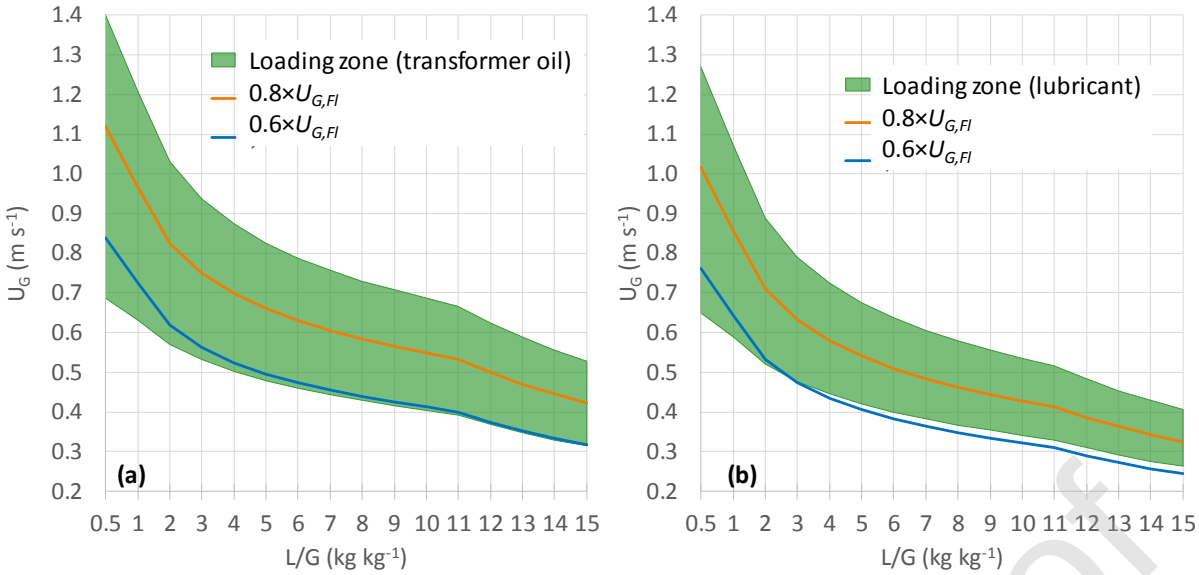

Figure 3: Evolution of the loading and flooding gas velocity for transformer oil (a) and lubricant (b) for increasing values of the *L/G* ratio (Flexipac® 500Z HC). The green frame corresponds to the loading zone (located between the loading and the flooding velocities). The orange and blue lines correspond to 80% and 60% of the flooding velocity, respectively. These data were simulated using the B-S correlations.

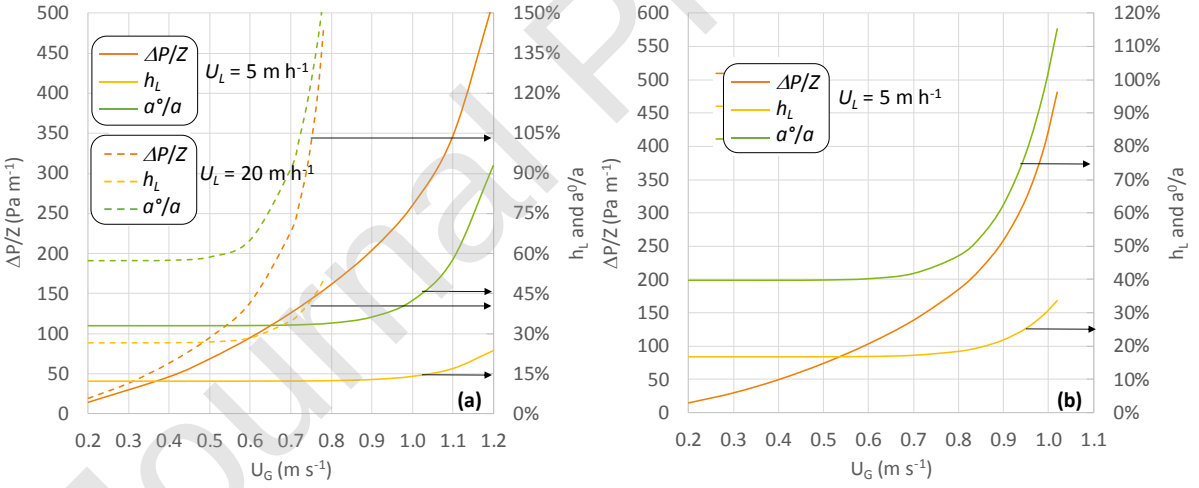

Figure 4: Evolution of the pressure drop (orange curves), the liquid holdup (yellow curves) and the ratio *a°/a* (green curves) for increasing values of the gas velocity for transformer oil (a) and lubricant (b) (Flexipac® 500Z HC). Two liquid loads (5 and 20 m h^{-1}) were simulated for the transformer oil and one liquid load (5 m h^{-1}) was simulated for the lubricant. These data were simulated using the B-S correlations.

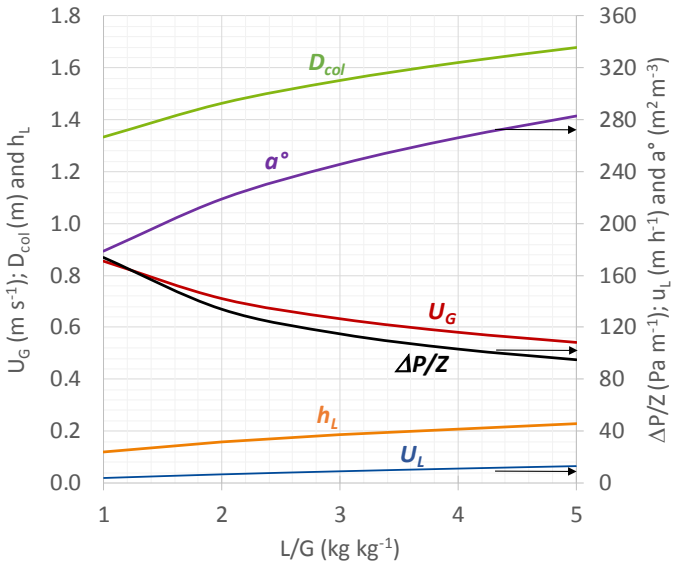

Figure 5: Evolution of the pressure drop (black curve), the liquid holdup (orange curve), the interfacial area *a*° (purple curve), the column diameter (green curve) and the liquid (blue curve) and gas (red curve) velocities for increasing values of the *L/G* ratio for the transformer oil for the following design: F_G = 4000 Nm^3 h^{-1}, $U_G = 0.80 \times U_{G,FI}$, using Flexipac® 500Z HC and ρ_G = 1.17 kg m^{-3}.

Table 1: Properties of the studied liquid absorbents.

Chemical composition	Siloxanes	Linear alkanes	
Dynamic viscosity μ_L (mPa s) at 25°C	20	19	79
Molar mass (g mol^{-1})	3000	212*	
Density ρ_L (kg m^{-3})	900	865	875
Superficial tension σ_L (N m^{-1})	0.021	0.027	0.031

* Lubricant and transformer oil have complex chemical structures. Several samples were investigated by ^{1}H-NMR spectroscopy and showed quite similar chemical natures between lubricant and transformer oil and allowed to roughly estimate an average chain length of 15 carbons which is coherent with literature data for mineral oils (Aluyor and Ori-jesu, 2009).

Table 2: Packing characteristics

Flexipac® 500Z HC	$7.60.10^{-3}$	500	0.95

Table 3: Operating conditions

bar	°C	m	m	Nm^3 h^{-1}	L h^{-1}	m s^{-1}	m s^{-1}
1	25	0.12	1	9 – 50	15 – 750	0.2 – 1.2	3.10^{-4} – 2.10^{-2}

Table 4: Billet-Schultes correlations developed for the determination of the parameters relative to the hydrodynamics of an irrigated counter-current packed column (Billet and Schultes, 1999, 1995, 1993, 1991).

Determination of the loading point ($U_{G,Lo}$) for a given *L/G* ratio	
$U_{G,Lo} = \sqrt{\frac{g}{\psi_{Lo}}} \times (\varepsilon - h_{L,Lo}) \times \sqrt{\frac{h_{L,Lo}}{a}} \times \sqrt{\frac{\rho_L}{\rho_G}}$	Eq. 1
$U_{L,Lo} = \frac{\rho_G}{\rho_L} \times \frac{L}{G} \times U_{G,Lo}$	Eq. 2
With:	
$\psi_{Lo} = \frac{g}{{C_{Lo}}^2} \times \left(\frac{L}{G}.\sqrt{\frac{\rho_G}{\rho_L}}\left(\frac{\mu_L}{\mu_G}\right)^{0.4}\right)^{0,752}$ if $\frac{L}{G} \times \sqrt{\frac{\rho_G}{\rho_L}} \leq 0.4$ (liquid dispersed in the gas)	Eq. 3
$\psi_{Lo} = \frac{g}{\left(0.695 C_{Lo}\left(\frac{\mu_L}{\mu_G}\right)^{0.1588}\right)^2} \times \left(\frac{L}{G}\sqrt{\frac{\rho_G}{\rho_L}}\left(\frac{\mu_L}{\mu_G}\right)^{0.4}\right)^{1,46}$ if $\frac{L}{G} \times \sqrt{\frac{\rho_G}{\rho_L}} > 0.4$ (gas dispersed in the liquid)	Eq. 4
And:	
$h_{L,Lo} = \left(\frac{12}{g}\frac{\mu_L}{\rho_L}a^2 U_{L,Lo}\right)^{1/3} \times \left(\frac{a_h}{a}\right)^{2/3}$	Eq. 5
With:	
$\left(\frac{a_h}{a}\right) = C_h \times \left(\frac{U_{L,Lo}.\rho_L}{a.\mu_L}\right)^{0.15} \times \left(\frac{{U_{L,Lo}}^2.a}{g}\right)^{0.1}$ if $\left(\frac{U_{L,Lo}.\rho_L}{a.\mu_L}\right) < 5$	Eq. 6
$\left(\frac{a_h}{a}\right) = 0.85 \times C_h \times \left(\frac{U_{L,Lo}.\rho_L}{a.\mu_L}\right)^{0.25} \times \left(\frac{{U_{L,Lo}}^2.a}{g}\right)^{0.1}$ if $\left(\frac{U_{L,Lo}.\rho_L}{a.\mu_L}\right) \geq 5$	Eq. 7
Determination of the flooding point ($U_{G,Fl}$) for a given *L/G* ratio	
$h_{L,Fl}^3.(3.h_{L,Fl} - \varepsilon) = \frac{6}{g}.a^2.\varepsilon.\frac{\mu_L}{\rho_L}.\frac{L}{G}.\frac{\rho_G}{\rho_L}.U_{G,Fl}$	Eq. 8
With:	
$U_{G,Fl} = \sqrt{\frac{2.g}{\psi_{Fl}}} \times \frac{(\varepsilon - h_{L,Fl})^{1.5}}{\varepsilon^{0.5}} \times \sqrt{\frac{h_{L,Fl}}{a}} \times \sqrt{\frac{\rho_L}{\rho_G}}$	Eq. 9
And:	
$\psi_{Fl} = \frac{g}{{C_{Fl}}^2}.\left(\frac{L}{G}\sqrt{\frac{\rho_G}{\rho_L}}\left(\frac{\mu_L}{\mu_G}\right)^{0.2}\right)^{0,388}$ if $\frac{L}{G} \times \sqrt{\frac{\rho_G}{\rho_L}} \leq 0.4$	Eq. 10
$\psi_{Fl} = \frac{g}{\left(0.6244 C_{Fl}\left(\frac{\mu_L}{\mu_G}\right)^{0.1028}\right)^2} \times \left(\frac{L}{G}\sqrt{\frac{\rho_G}{\rho_L}}\left(\frac{\mu_L}{\mu_G}\right)^{0.2}\right)^{1.416}$ if $\frac{L}{G} \times \sqrt{\frac{\rho_G}{\rho_L}} > 0.4$	Eq. 11
Determination of the holdup (h_L) at the working point ($U_G < U_{G,Fl}$ and $U_L = \frac{\rho_G}{\rho_L}.\frac{L}{G}.U_G$)	
Step 1: $h_{L,Lo}$ from Eqs. 5-7 and calculated with U_L	Eq. 12
Step 2: $h_{L,Fl} = 2.2 h_{L,Lo}\left(\frac{\mu_L \rho_W}{\mu_W \rho_L}\right)^{0.05}$	Eq. 13
Step 3: $h_L = h_{L,Lo} + (h_{L,Fl} - h_{L,Lo}) \times \left(\frac{U_G}{U_{G,Fl}}\right)^{13}$ (with $h_{L,Lo}$ and $h_{L,Fl}$ from steps 1 and 2)	Eq. 14
Determination of the pressure drop ($\Delta P/Z$) at the working point	
$\frac{\Delta P}{Z} = \psi_L \times \frac{a}{(\varepsilon - h_L)^3} \times \frac{{U_G}^2 \rho_G}{2} \times \left(1 + \frac{4}{aD_{col}}\right)$	Eq. 15
With:	
$\psi_L = C_P \times \left(\frac{64}{Re_G} + \frac{1.8}{{Re_G}^{0.08}}\right) \times exp\left(\frac{13300}{a}.\sqrt{\frac{U_L^2}{g}}\right) \times \left(\frac{\varepsilon - h_L}{\varepsilon}\right)^{1.5} \times \left(\frac{h_L}{h_{L,Lo}}\right)^{0.3}$ with h_L and $h_{L,Lo}$ calculated from Eqs. 12 and 14	Eq. 16
$Re_G = \frac{6}{a}\frac{U_G \rho_G}{\mu_G}\left(1 + \frac{4}{aD_{col}}\right)^{-1}$	Eq. 17
Determination of the interfacial area ($a°$) at the working point	

Step 1: $\left(\frac{a^\circ}{a}\right)_{Lo} = 1.5(ad_h)^{-0.5}\left(\frac{U_L d_h \rho_L}{\mu_L}\right)^{-0.2}\left(\frac{{U_L}^2 d_h \rho_L}{\sigma_L}\right)^{0.75}\left(\frac{{U_L}^2}{g d_h}\right)^{0.45}$ in which U_L is the working liquid velocity	Eq. 18
Step 2: $\left(\frac{a^\circ}{a}\right)_{Fl} = 7\left(\frac{a^\circ}{a}\right)_{Lo}\left(\frac{\sigma_L}{\sigma_W}\right)^{0.56}$	Eq. 19
Step 3: $\left(\frac{a^\circ}{a}\right) = \left(\frac{a^\circ}{a}\right)_{Lo} + \left(\left(\frac{a^\circ}{a}\right)_{Fl} - \left(\frac{a^\circ}{a}\right)_{Lo}\right) \times \left(\frac{U_G}{U_{G,Fl}}\right)^{13}$ (with $\left(\frac{a^\circ}{a}\right)_{Lo}$ and $\left(\frac{a^\circ}{a}\right)_{Fl}$ from steps 1 and 2)	Eq. 20

Table 5. Comparison of the experimental loading gas velocities ($U_{G,Lo}$) at a given liquid load (U_L) and *L/G* ratio to the ones predicted using the Billet-Schultes correlations (Eqs 1-7). *RE* corresponds to the relative error between the experimental and the theoretical loading gas superficial velocities. The liquid holdup ($h_{L,Lo}$) determined with the Billet-Schultes correlations is also provided.

	U_L (m h^{-1})	*L/G*	$U_{G,Lo}$ experimental (m s^{-1})	$U_{G,Lo}$ model (m s^{-1})	*RE*	$h_{L,Lo}$ model
PDMS	3.06	1.02	0.64	0.64	0.0%	0.092
	7.38	2.81	0.56	0.55	2.4%	0.150
	12.36	5.50	0.48	0.48	0.5%	0.203
	23.65	12.95	0.39	0.36	8.2%	0.280
Transformer oil	9.92	3.18	0.64	0.53	17.8%	0.160
	16.14	5.92	0.56	0.46	17.6%	0.211
Lubricant	1.40	0.45	0.65	0.66	1.2%	0.083
	2.69	1.00	0.56	0.59	5.0%	0.122
	3.97	1.72	0.48	0.54	11.6%	0.158
	5.23	2.53	0.43	0.50	15.3%	0.188

Table 6. Comparison of the experimental flooding gas velocities ($U_{G,FI}$) at given liquid load (U_L) and *L/G* ratio to the ones predicted using the Billet-Schultes correlations (Eqs 8-11). *RE* corresponds to the relative error between the experimental and the theoretical flooding gas superficial velocities. The liquid holdup ($h_{L,FI}$) determined with the Billet-Schultes correlations is also provided.

	U_L (m h^{-1})	*L/G*	$U_{G,FI}$ experimental (m s^{-1})	$U_{G,FI}$ model (m s^{-1})	RE	$h_{L,FI}$ model
PDMS	17.81	3.59	1.06	0.92	13.4%	0.3927
	23.65	6.24	0.81	0.80	1.5%	0.4145
	29.82	8.72	0.73	0.73	0.1%	0.4293
	36.27	13.83	0.56	0.58	3.5%	0.4445
Transformer oil	16.14	3.38	0.98	0.91	7.1%	0.3909
	22.79	5.78	0.81	0.80	1.7%	0.4116
	29.78	9.40	0.65	0.70	7.5%	0.4331
Lubricant	6.48	1.26	1.07	1.00	5.7%	0.4181
	7.71	1.95	0.82	0.90	9.2%	0.4382
	8.94	2.54	0.73	0.83	13.7%	0.4511
	10.16	3.25	0.65	0.77	19.0%	0.4637

Table 7: Billet-Schultes constants determined and comparison with the ranges determined by the authors for other packing materials.

Flexipac® 500Z HC	500	0.95	0.462	1.68	1.50	1.73
Range of B-S correlations (Billet and Schultes, 1999)	80-545	0.68-0.985	0.25-1.33	2.45-3.79	0.482-1.90	1.55-3.02

Table 8: *ARE* between the experimental and theoretical (B-S correlations) pressure drops for the three solvents studied in the pre-loading and loading zones.

PDMS 20			**Transformer oil**			**Lubricant**		
Both zones	Pre-loading zone	Loading zone	Both zones	Pre-loading zone	Loading zone	Both zones	Pre-loading zone	Loading zone
17.9%	31.8%	12.1%	19%	32%	13%	27%	36%	20%